THE JOURNAL OF BIOLOGICAL CHEMISTRY VOL. 289, NO. 16, pp. 10975–10987, April 18, 2014
© 2014 by The American Society for Biochemistry and Molecular Biology, Inc. Published in the U.S.A.

Blocking Metabotropic Glutamate Receptor Subtype 7 (mGlu7) via the Venus Flytrap Domain (VFTD) Inhibits Amygdala Plasticity, Stress, and Anxiety-related Behavior◆

Received for publication, December 12, 2013, and in revised form, February 19, 2014 Published, JBC Papers in Press, March 4, 2014 DOI 10.1074/jbc.M113.542654

Christine E. Gee[‡§1], Daniel Peterlik[¶1], Christoph Neuhäuser[¶], Rochdi Bouhelal[‡], Klemens Kaupmann[‡], Grit Laue[‡], Nicole Uschold-Schmidt[¶], Dominik Feuerbach[‡], Kaspar Zimmermann[‡], Silvio Ofner[‡], John F. Cryan[‡‖], Herman van der Putten[‡], Markus Fendt[‡], Ivo Vranesic[‡], Ralf Glatthar[‡2], and Peter J. Flor[‡¶3]**

*From the [‡]Novartis Institutes for BioMedical Research, Novartis AG, CH-4057 Basel, Switzerland, the [§]Center for Molecular Neurobiology Hamburg, University Medical Center Hamburg-Eppendorf, D-20249 Hamburg, Germany, the [¶]Faculty of Biology and Preclinical Medicine, Laboratory of Molecular and Cellular Neurobiology, University of Regensburg, D-93053 Regensburg, Germany, the [‖]Department of Anatomy and Neuroscience, University of Cork, Cork, Ireland, and the **Institute of Pharmacology and Toxicology and Center of Behavioral Brain Sciences, University of Magdeburg, D-39120 Magdeburg, Germany*

Background: Behavioral genetics identified mGlu7 as a key regulator of brain emotion circuits.
Results: An mGlu7-selective, Venus flytrap domain (VFTD)-directed antagonist inhibits fear, synaptic plasticity, stress, and anxiety in rodents.
Conclusion: Pharmacological blockers of mGlu7 may represent promising future anxiolytics and antidepressants in man.
Significance: The VFTD region of class C GPCRs provides a promising target for computer-assisted drug design.

The metabotropic glutamate receptor subtype 7 (mGlu7) is an important presynaptic regulator of neurotransmission in the mammalian CNS. mGlu7 function has been linked to autism, drug abuse, anxiety, and depression. Despite this, it has been difficult to develop specific blockers of native mGlu7 signaling in relevant brain areas such as amygdala and limbic cortex. Here, we present the mGlu7-selective antagonist 7-hydroxy-3-(4-iodophenoxy)-4*H*-chromen-4-one (XAP044), which inhibits lateral amygdala long term potentiation (LTP) in brain slices from wild type mice with a half-maximal blockade at 88 nM. There was no effect of XAP044 on LTP of mGlu7-deficient mice, indicating that this pharmacological effect is mGlu7-dependent. Unexpectedly and in contrast to all previous mGlu7-selective drugs, XAP044 does not act via the seven-transmembrane region but rather via a binding pocket localized in mGlu7's extracellular Venus flytrap domain, a region generally known for orthosteric agonist binding. This was shown by chimeric receptor studies in recombinant cell line assays. XAP044 demonstrates good brain exposure and wide spectrum anti-stress and antidepressant- and anxiolytic-like efficacy in rodent behavioral paradigms. XAP044 reduces freezing during acquisition of Pavlovian fear and reduces innate anxiety, which is consistent with the phenotypes of mGlu7-deficient mice, the results of mGlu7 siRNA knockdown studies, and the inhibition of amygdala LTP by XAP044. Thus, we present an mGlu7 antagonist with a novel molecular mode of pharmacological action, providing significant application potential in psychiatry. Modeling the selective interaction between XAP044 and mGlu7's Venus flytrap domain, whose three-dimensional structure is already known, will facilitate future drug development supported by computer-assisted drug design.

G protein-coupled receptors (GPCRs)[4] in vertebrates constitute a superfamily of 1000–2000 cell surface proteins. GPCRs can be activated by a large and diverse array of extracellular signals, including photons, ions, hormones, pheromones, growth factors, and peptide neuromodulators, and classical neurotransmitters, such as catecholamines and amino acids. GPCRs also represent the largest class of drug targets for registered medicines. Generally, GPCRs are seven-transmembrane receptors that transduce signals primarily by activating G proteins, activating second messengers, and modulating ion channels (1–3). Based on phylogenetics and protein sequence similarity, GPCRs are classified into three major classes (A, B, and C). Class C GPCRs are involved in a wide variety of physiological processes, and their ligands include pheromones, calcium, nutrients, GABA, and L-glutamate. These ligands bind their cognate receptors via a large (~600 amino acids) N-terminal extracellular domain with cysteine-rich regions and a Venus flytrap domain (VFTD) (2, 4, 5). The large N-terminal extracellular domain is connected to a seven-transmembrane region

◆This article was selected as a Paper of the Week.

[1] Both authors contributed equally to this work.
[2] To whom correspondence may be addressed: Novartis Pharma AG, CH-4057 Basel, Switzerland. Tel.: 4161-696-8471; Fax: 4161-696-2455; E-mail: ralf.glatthar@novartis.com.
[3] Supported by Grant FL 729/2-1 from the German Research Foundation. To whom correspondence may be addressed: Faculty of Biology and Preclinical Medicine, University of Regensburg, D-93053 Regensburg, Germany. Tel.: 49-941-3079; Fax: 49-941-3052; E-mail: peter.flor@biologie.uni-regensburg.de.

[4] The abbreviations used are: GPCR, G protein-coupled receptor; VFTD, venus flytrap domain; mGlu, metabotropic glutamate receptor; NAM, negative allosteric modulator; EPM, elevated plus-maze; MMPIP, 6-(4-methoxyphenyl)-5-methyl-3-pyridin-4-ylisoxazolo[4,5-c]pyridin-4(5*H*)-one; LTP, long term potentiation; LA, lateral amygdala; TST, tail suspension test; PK, pharmacokinetic; SIH, stress-induced hyperthermia; MPEP, 2-methyl-6-(phenylethynyl)pyridine; V1a, arginine vasopressin receptor 1a; fEPSP, field excitatory post-synaptic potential; p.o., oral; ANOVA, analysis of variance; GTPγS, guanosine 5′-3-*O*-(thio)triphosphate; lx, lux.

(~260 amino acids) followed by an intracellular C-terminal domain consisting of 30–300 amino acids. Downstream signaling is activated by ligand binding to the VFTD, which induces conformational changes that result in a closing of the two lobes and a propagation of the signal via the extracellular cysteine-rich domain and the transmembrane and cytoplasmic domains (3, 6, 7).

L-Glutamate, the main excitatory neurotransmitter in the mammalian brain, activates eight subtypes of metabotropic glutamate receptors (mGlu1–8) that belong to class C GPCRs. Based on sequence homology, signal transduction, and pharmacology, mGlu1–8 have been classified into three groups (I–III). We and others have focused on elucidating physiological roles of the group III receptor mGlu7, evolutionarily the most highly conserved mGlu subtype, suggesting it plays a key role in brain and synaptic function (7–9). Supporting a key role in brain physiology, mice lacking mGlu7 were shown to have deficits in amygdala-dependent fear learning and aversive behavior (10), reduced anxiety- and depression-like behavior (11–14), and alterations in stress responses, including elevated production of brain-derived neurotrophic factor in the hippocampus (15). At the synaptic level, mGlu7 appears to regulate presynaptic GABA and L-glutamate release, which may contribute to mGlu7's regulating role in emotion-relevant brain circuitry (14, 16, 17). This role is also supported by findings in mice using siRNA-induced knockdown of mGlu7, inducing changes in innate anxiety, physiological and behavioral stress responses, and fear learning (18). Brain-penetrable, low molecular weight compounds that can block mGlu7 function are needed to substantiate these findings in animals and pave the road for possible clinical applications in psychiatry.

Unfortunately, the discovery and development of compounds specifically targeting mGlu7 and suitable for probing its role *in vivo* is lagging years behind the successful discovery and clinical testing of drugs acting at the group II mGlu2/3 and group I mGlu5 subtypes (19). The first mGlu7-selective allosteric agonist *N,N′*-dibenzhydrylethane-1,2-diamine dihydrochloride (AMN082) has induced both anxiogenic-like (15, 20), as well as anxiolytic-like and antidepressant-like behavioral responses in rodents (13, 14, 21–23). However, the latter effects seem in contradiction with anxiolytic- and antidepressant-like behavioral changes observed in mice lacking mGlu7 or after siRNA-mediated knockdown. Also, AMN082 has been shown to induce a rapid and long-lasting internalization of mGlu7 receptors, which could translate into functional antagonism of the receptor (24). Furthermore, the primary metabolite of AMN082, *N*-benzhydrylethane-1,2-diamine, inhibits serotonin and norepinephrine reuptake transporters (24, 25). Altogether, these findings may explain the seemingly conflicting results obtained using AMN082 *in vivo*.

Like AMN082, two systemically active mGlu7 negative allosteric modulators (NAMs) have yielded disparate results in behavioral paradigms despite displaying very similar pharmacological properties *in vitro*. ADX71743 (26) was shown to have robust anxiolytic-like effects in the elevated plus-maze (EPM) and the marble burying test. In contrast, MMPIP (27–29) showed no effects in a battery of anxiety-like and depression-related tests but was active in spatial learning tasks. Like AMN082, both NAMs likely act via allosteric sites in more lipophilic domains rather than at the VFTD. Increased lipophilicity of compounds may be associated with undesirable off-target effects. Furthermore, single and/or different allosteric ligands do not necessarily affect all downstream signaling pathways of a given GPCR (30).

To advance our understanding of mGlu7 function and its therapeutic implications, better tool compounds are needed that ideally target a more hydrophilic binding pocket of the receptor. Here, we present 7-hydroxy-3-(4-iodophenoxy)-4*H*-chromen-4-one (XAP044), which we identified via a high throughput screening effort. XAP044 is the first mGlu7-selective antagonist that binds within the VFTD close to the binding site of the orthosteric agonist L-glutamate. We show that in brain slices XAP044 blocks long term potentiation (LTP) in the lateral amygdala (LA), an assay that is considered an *in vitro* electrophysiological correlate of fear learning. Furthermore, XAP044 demonstrates a broad spectrum of anti-stress and antidepressant- and anxiolytic-like effects in mice that are consistent with effects observed in mGlu7 knock-out mice and siRNA-mediated knockdown experiments. Because several three-dimensional structures of VFTD regions are known (31–35), our findings pave the way to structure-based design of novel compounds targeting mGlu7 and also to more specific and powerful pharmacological agents to probe mGlu7 function in the clinic. Antagonists targeting the VFTD region of class C GPCRs might prove generally applicable to the design of drugs for this class of receptors.

EXPERIMENTAL PROCEDURES

Animals—For *in vivo* testing, male C57BL/6 mice (from Charles River, Sulzfeld, Germany, for tail suspension test (TST), EPM, and fear conditioning, and from Iffa-Credo, France, for pharmacokinetic (PK) study), male Sprague-Dawley rats (Iffa Credo, France, for PK study), and male OF1 mice (from Novartis Pharma AG, Basel, Switzerland, and Charles River, L'Arbresle, France, for stress-induced hyperthermia (SIH) test) were used. For electrophysiological recordings, male wild type mice and their mGlu7 receptor knock-out littermates on a C57BL/6 background were used as described previously (12). All mice were individually housed and kept under standard laboratory conditions (12:12-h light/dark cycle, lights on at 0600 h, 22 °C, 60% humidity, water and food available *ad libitum*). All experimental protocols were approved by the Committee on Animal Health and Care of the respective local governments and performed according to international guidelines on the ethical use of animals. All efforts were made to minimize the number of animals used and their suffering.

Drugs and Material—XAP044 (identified by high throughput random drug screening and follow-up chemical efforts), D-(*E*)-2-amino-4-methyl-5-phosphono-3-pentenoic acid (CGP40116), AMN082, MPEP, and chlorodiazepoxide were synthesized at Novartis Pharma AG (Basel, Switzerland). L-Glutamate, DL-2-amino-4-phosphonobutyric acid (DL-AP4). GABA, and 2-[(1*S*,2*S*)-2-carboxycyclopropyl]-3-(9*H*-xanthen-9-yl)-D-alanine (LY341495) were purchased from Tocris (Anawa Trading SA, Zürich, Switzerland). Forskolin and imipramine were obtained from Sigma-Aldrich. Diazepam was obtained from

Ratiopharm GmbH (Ulm, Germany). Drugs were dissolved in 10% Neoral® vehicle (Novartis Pharma AG, Basel, Switzerland) and diluted in 0.4% methylcellulose (AMIMED, Allschwill, Switzerland) except for electrophysiological recordings, where XAP044 and CGP40116 were dissolved at greater than 1000-fold final concentration in 100% DMSO (Merck) and diluted to final working concentrations just before use. All other chemicals were of reagent grade and obtained from Fluka (Buchs, Switzerland), Merck, Serva (Heidelberg, Germany), or Sigma-Aldrich.

Stable Mammalian Cell Lines—Generation, culture, and pharmacological characterization of stable CHO or L cell lines transfected with mammalian mGlu2, mGlu4, mGlu5a, mGlu6, mGlu6/7, mGlu7a, mGlu7b, mGlu7/5a, mGlu7/6, $GABA_B$, arginine vasopressin 1A (V1a), and oxytocin receptors were conducted as described recently (8, 22, 36–39).

Construction of Chimeric Receptors—cDNAs encoding human mGlu6 and mGlu7b were described previously (8, 40). cDNAs encoding chimeric human mGlu6/7b, mGlu7/6, and mGlu7/5a were constructed by using the polymerase chain reaction overlap extension approach (39, 41). The mGlu6/7b construct contains 570 amino acids derived from the N-terminal VFTD region of mGlu6 and the remaining C-terminal portion of mGlu7b, comprising the entire transmembrane domain and C-terminal intracellular region. mGlu7/6 is essentially the reverse chimera with the fusion point at amino acid 575. The mGlu7/5a construct contains 865 amino acids derived from the N-terminal extracellular and transmembrane regions of mGlu7 and the remaining C-terminal intracellular portion of mGlu5a.

[^{35}S]GTPγS Binding Assays—[^{35}S]GTPγS binding assays were conducted according to the protocol described by Maj *et al.* (42) using membranes prepared from CHO cells stably transfected with individual receptor genes.

Second Messenger Assays—Measurements of cAMP accumulation and intracellular Ca^{2+} responses were performed essentially as described previously (8, 36, 42–44) using CHO and L cells stably expressing individual receptor genes.

Electrophysiological Recordings—Preparation of acute brain slices containing the amygdala and subsequent field recordings were performed as described previously (14, 45). Male C57BL/6 mice were used to test the dose dependence of XAP044, and male wild type (*Grm7*$^{+/+}$) and knock-out (*Grm7*$^{-/-}$) littermate mice ((46), $F > 10$ backcrossed to C57BL/6) were used to test for potential off-target effects of XAP044 on LTP. Mice were anesthetized with isoflurane and sacrificed by decapitation. The skull covering the cortex was removed, and the brain was quickly excised and placed in ice-cold artificial cerebrospinal fluid equilibrated with 95% O_2, 5% CO_2 containing (in mM) the following: NaCl (124), KCl (2.5), KH_2PO_4 (1.2), $CaCl_2$ (2.5), $MgSO_4$ (1.3), $NaHCO_3$ (26), glucose (10), and saccharose (4). Osmolarity was adjusted to 320 ± 2 mosM by reducing the amount of H_2O, and pH was set to 7.4. Coronal slices (350–400 μM thick) containing the amygdala complex were cut on a vibrating microtome and maintained until use (at least 1 h) at room temperature in the fully diluted artificial cerebrospinal fluid (osmolarity 306 ± 2 mosM). Field recordings were made in an interface-type recording chamber and superfused with solution containing 5 μM picrotoxin (to partially block inhibition) at 27 °C. Twisted nichrome wire (50 μM diameter) stimulation electrodes were positioned to activate thalamic inputs, and glass recording electrodes (filled with 4 M NaCl, 3–5 megohms) were used to record field excitatory post-synaptic potentials (fEPSPs) from the LA (47). Responses were recorded with an Axoprobe 1A amplifier and pClamp 9.0 software (Molecular Devices, Biberach an der Riss, Germany). Test stimuli were delivered at an intensity to evoke an fEPSP 25–40% of maximum every 20 s. After recording a stable baseline for at least 10 min in the presence of vehicle (DMSO) or a compound (XAP044 or CGP40116), LTP was induced with five 1-s trains of 100 Hz stimuli delivered every 20 s. Control and drug experiments were interleaved. Wild type and knock-out mice were littermates, and experiments and analyses using slices from transgenic animals were performed blind to genotype. The fEPSP slope was measured and data were normalized to the average baseline fEPSP slope for each slice. The average fEPSP slope was calculated for the interval 30–40 min after LTP induction.

PK Studies—To estimate exposure of XAP044 in pharmacological studies in mice, plasma and brain concentrations of XAP044 were determined after intraperitoneal administration of XAP044 to mice at 10 and 100 mg/kg, dosed in 10% Neoral® vehicle, 0.4% methylcellulose at 10 ml/kg. Plasma and brain samples were collected after decapitation 30 min after dosing. The brain samples were homogenized with 2 mM KH_2PO_4 buffer. Brain homogenate and plasma samples were subjected to protein precipitation with acetonitrile, and aliquots of the samples were injected into the LC/MS/MS system (CTC PAL autosampler, Rheos Allegro LC pump, LTQ XL MS, all from Thermo Scientific, Waltham, MA). XAP044 was separated from potential metabolites and endogenous matrix components on a Discovery® HS F5 HPLC column using a gradient elution with 1% formic acid in water, 1% formic acid in acetonitrile/methanol (50:50 v/v). XAP044 was detected in negative electrospray mode using the MS/MS transition from the deprotonated parent mass to a specific daughter ion (379 to 252 Da). The limit of detection was 5 nM in plasma and 15 nmol/kg in brain.

Full pharmacokinetic profiles in mice and rats were obtained for XAP044 after intravenous (i.v.) and oral (p.o.) administration (Table 1). XAP044 was dosed in male C57BL/6 mice in a cassette approach with five structurally similar compounds. A reference compound with known PK properties was always included to validate the cassette dosing. For i.v. injection, 1 mg/kg of each test compound was individually solubilized in *N*-methylpyrrolidone, mixed together, and diluted in blank plasma. The final formulation mixture (NMP/blank plasma, 10:90 v/v) was administered at 5 ml/kg body weight into the saphenous vein. For oral dosing, 3 mg/kg of each test compound was individually suspended in carboxymethylcellulose, 0.5% w/v, in water/Tween 80 (99.5:0.5%, v/v); suspensions were mixed together and applied by oral gavage at 2.5 ml/kg body weight. Blood was collected by sublingual bleeding or at sacrifice at 5 (i.v.), 15 (p.o.), and 30 min and 1, 2, 4, 6, 8, and 24 h per day. The PK profile of XAP044 in rats was obtained by single compound dosing in dual-cannulated male Sprague-Dawley

rats. For i.v. administration, XAP044 was administered at 3 mg/kg in NMP/PEG200 (30:70, v/v) at 0.5 ml/kg body weight into the femoral vein, and for p.o. administration, the compound was suspended in carboxymethylcellulose, 0.5% w/v, in water/Tween 80 (99.5:0.5%, v/v) and was dosed via oral gavage at 10 mg/kg (2 ml/kg body weight). Plasma was generated from blood collected serially from the femoral artery at the same time points as described for mice.

The absorption and disposition parameters were estimated by a noncompartmental analysis using the mean blood concentration ($n = 3$) *versus* time profiles after p.o. and i.v. administration. The apparent terminal phase rate constant was determined by choosing the last three data points from the log linear regression of the blood concentrations *versus* time curve and was used for the extrapolation of the area under the curve to infinity. The absolute oral bioavailability was calculated by dividing the dose-normalized area under the curve after p.o. administration by the respective area under the curve after i.v. administration assuming linear pharmacokinetics between the intravenous and oral doses, respectively.

In Vitro Testing, Binding to Plasma Proteins in Mice and Rats and to Rat Brain Homogenate—The free fraction in mouse and rat plasma as well as in rat brain homogenate was assessed by rapid equilibrium dialysis applying a slightly adapted literature method (48).

In Vivo Testing, SIH Test—SIH was performed in mice individually housed in small macrolon cages as described previously (18). Briefly, mice were injected intraperitoneally with vehicle (10% Neoral® vehicle, 0.4% methylcellulose), chlorodiazepoxide (10 mg/kg) as positive control, or XAP044 (10, 30, and 60 mg/kg) 30 min before recording rectal temperature. Rectal temperature was then recorded twice at $t1$ (30 min after intraperitoneal injection) and $t2$ (45 min after intraperitoneal injection). Recording of $t1$ indicates baseline temperature and served as stressor. Recording of $t2$ allows determination of SIH defined as the difference between $t2$ and $t1$.

In Vivo Testing, TST—The TST, a well characterized test for assessing depressive-like behavior (12, 49, 50), was performed as described previously (51). Mice were injected intraperitoneally with vehicle (10% Neoral® vehicle, 0.4% methylcellulose), imipramine (20 mg/kg) as positive control, or XAP044 (10 and 60 mg/kg). Thirty min later, mice were individually suspended by the tail to a vertical ring-stand bar (distance from floor = 40 cm) using adhesive tape (distance from tip of tail = 2 cm). Typically, the animals demonstrated several escape-oriented behaviors with temporally increasing periods of immobility. A 6-min test session was employed, which was videotaped and subsequently analyzed for the time the mice spent immobile (seconds) by a trained observer blind to the treatment.

In Vivo Testing, Elevated Plus-maze (EPM) Test—Anxiety-related behavior was assessed using the EPM test as described previously (52). EPM testing took place for 5 min. The mouse plus-maze consists of two open (6 × 30 cm, 140 lx) and two closed (6 × 30 × 17 cm, 25 lx) arms radiating from a central platform (6 × 6 cm) to form a plus-shaped figure elevated 130 cm above the floor. The open arm edges were 0.3 cm in height to avoid falling. Thirty min after i.p. injection of vehicle (10% Neoral® vehicle, 0.4% methylcellulose), diazepam (1 mg/kg) as positive control, or XAP044 (10 and 60 mg/kg), each mouse was placed on the central platform facing a closed arm. The entries into the open and closed arms were recorded by means of a video/computer setup (Plus-maze, DOS program, E. Fricke, 1993, Munich, Germany) to allow calculation of the ratio open/total arm entries of the maze. The number of total arm entries was taken as the indicator for locomotor activity. The maze was thoroughly cleaned before each test.

In Vivo Testing, Fear Conditioning Paradigm—To measure the conditioned freezing response in mice, a computerized fear-conditioning system (TSE, Bad Homburg, Germany) was used as described previously (14, 18, 53). The cued-fear experiments were performed in two different contexts, A and B, that differed in visual, tactile, and olfactory cues. On day 1, fear acquisition was assessed in context A, which consisted of a transparent perspex box (45 × 45 × 40 cm) with a transparent lid. The floor was made up of 45 × 0.4-m stainless steel bars set 0.5 cm apart, which served as conductors of mild foot shocks; 30 min after intraperitoneal injection of vehicle (10% Neoral® vehicle, 0.4% methylcellulose), MPEP (30 mg/kg) as positive control, or XAP044 (10 and 60 mg/kg), each mouse was individually placed into the conditioning chamber and, after a 5-min adaptation period, exposed to five CS-US pairings. The conditioned stimulus (CS) was a white noise (80 db, 8 kHz, 30 s), which co-terminated with a mild electric food shock (US, 0.6 mA, 2 s). After the CS-US pairings, mice were left in the conditioning chamber for 5 min before they were returned to their home cage. Context A was cleaned with a neutral smelling detergent before each trial. On day 2, fear expression was evaluated in context B, which consisted of a black box (45 × 45 × 40 cm) with a smooth floor. After a 5-min adaptation period, the animals received two CS presentations (80 db, 8 kHz, 30 s) with an inter-stimulus interval of 30 s. Context B was cleaned with a lemon-scented detergent before each trial. Boxes were located in a wooden chamber to reduce external noise and visual stimulation, provided with loudspeakers for the acoustic stimuli, and ventilation fans producing a low background noise. Illumination (300 lx for context A and 20 lx for context B) was provided by four white LEDs. Movements of animals were detected by infrared sensors. In both the fear acquisition and the fear expression phases, the time spent freezing (immobility, no infrared beam crosses for more than 1 s) relative to the total time (set to 100%) was automatically recorded and defined as freezing response (%) (54).

Statistical Analysis—SIH, TST, and EPM test data were analyzed using a Kruskal-Wallis analysis of variance (ANOVA), each followed by a post hoc Dunnett's test when appropriate. Fear acquisition and fear expression data were analyzed using repeated measures ANOVA followed by a post hoc Fisher's least significant difference test when appropriate. Data of electrophysiological recordings were analyzed using two-tailed, paired, or unpaired t test. In all cases, significance was taken at $p < 0.05$.

RESULTS

Identification and in Vitro Pharmacology of XAP044—After a high throughput random drug screening campaign for mGlu7-selective ligands, subsequent hit confirmation, and lead optimi-

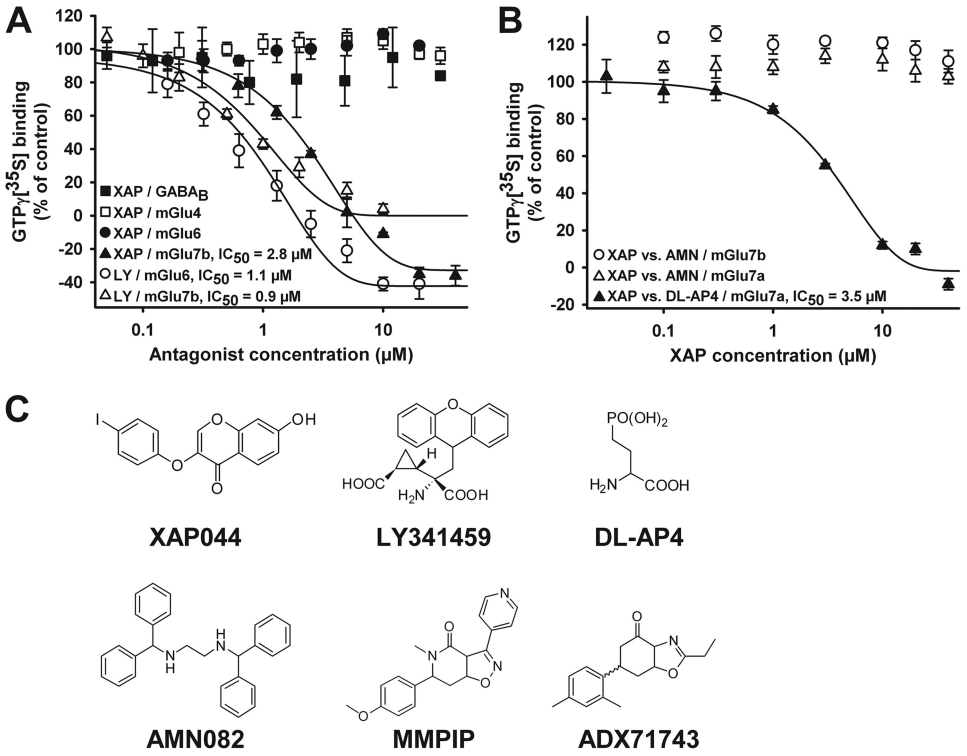

FIGURE 1. **XAP044 selectively antagonizes [^{35}S]GTPγS binding via mGlu7.** *A,* concentration-response curves for XAP044 (*XAP*) and LY341495 (*LY*) against agonist (EC_{90})-stimulated [^{35}S]GTPγS (*GTPγ[^{35}S]*) binding on membranes from CHO cells stably expressing either $GABA_B$, mGlu4, mGlu6, or mGlu7b. *B,* concentration-response curves for XAP044 using [^{35}S]GTPγS binding on membranes from CHO cells stably expressing mGlu7a or mGlu7b activated with AMN082 (*AMN*; 3 μM) or DL-AP4 (4 mM). All data points represent the mean ± S.E. from at least three independent measurements ($n \geq 3$) normalized to the control stimulation of near-maximal agonist concentrations (*e.g.* 4 mM DL-AP4 in the case of mGlu7, set to 100%). *C,* chemical structures of XAP044, LY341495, DL-AP4, AMN082, MMPIP, and ADX71743.

zation processes, XAP044 was identified. This compound revealed no structural resemblance to the broad spectrum mGlu antagonist LY341495, the orthosteric group III mGlu agonist DL-AP4, the allosteric mGlu7 activator AMN082, or the mGlu7 NAMs ADX71743 and MMPIP (Fig. 1*C*). XAP044's pharmacological properties and mechanism of action were further investigated using pharmacological assays, including [^{35}S]GTPγS binding, accumulation of cAMP, and determining intracellular Ca^{2+} levels.

A classical [^{35}S]GTPγS binding assay was performed with membranes prepared from CHO cells stably expressing either human mGlu4, mGlu6, mGlu7b, or $GABA_B$ receptors, and concentration-response curves were determined. The results showed that XAP044 selectively and dose-dependently reduced DL-AP4-induced (4 mM) activation of human mGlu7b (IC_{50} = 2.8 μM; Fig. 1*A*). In contrast, XAP044 had no effect on DL-AP4-induced activation of [^{35}S]GTPγS binding by mGlu4 and mGlu6 or on GABA-induced (50 μM) activation of [^{35}S]GTPγS binding by $GABA_B$ receptors. For comparison, the broad spectrum mGlu antagonist LY341495 dose-dependently reduced DL-AP4-induced activation of both human mGlu6 (IC_{50} = 1.1 μM) and mGlu7b (IC_{50} = 0.9 μM; Fig. 1*A*).

Next, we investigated whether binding of XAP044 to mGlu7 inhibits [^{35}S]GTPγS binding induced by different agonists. To this end, we tested agonists acting at either an allosteric (AMN082) or orthosteric site (DL-AP4) of mGlu7. Concentration-response curves were assessed for XAP044 in the presence of either AMN082 (3 μM, a near-maximal concentration) or in the presence of DL-AP4 (4 mM, a near-maximal concentration; Fig. 1*B*) using cell membranes expressing rat mGlu7a or human mGlu7b. Increasing concentrations of XAP044 only reduced DL-AP4-induced activation at mGlu7a (Fig. 1*B*) and mGlu7b (Fig. 1*A*), with IC_{50} = 2.8–3.5 μM, but AMN082-induced activation of mGlu7a or mGlu7b was not affected (Fig. 1*B*). These findings suggest that XAP044 may inhibit mGlu7 signaling by interfering specifically with orthosteric ligand binding in the VFTD, as XAP044 did not interfere with AMN082-mediated allosteric activation of mGlu7.

XAP044 Directly Interacts with the N-terminal Extracellular VFTD of mGlu7—To test whether XAP044 binds within the VFTD of mGlu7, we used cell lines expressing human mGlu7b, mGlu6, and two chimeric receptors. The latter receptors had either the extracellular N-terminal VFTD portion of mGlu7 fused to the transmembrane and C-terminal portion of mGlu6 (mGlu7/6 chimera) or the N-terminal extracellular region of mGlu6 fused to the transmembrane and C-terminal portion of mGlu7b (mGlu6/7 chimera; see under "Experimental Procedures," "Construction of Chimeric Receptors," and Fig. 2). Both XAP044 and the broad spectrum mGlu antagonist LY341495 dose-dependently inhibited human mGlu7b [^{35}S]GTPγS binding with IC_{50} values of 3.0 and 0.9 μM, respectively (Fig. 2*A*). LY341495, but not XAP044, reduced mGlu6 [^{35}S]GTPγS binding (IC_{50} = 0.4 μM; Fig. 2*B*), confirming the selectivity of XAP044 for mGlu7. The binding of [^{35}S]GTPγS binding by the human mGlu7/6 chimeric receptor, which harbors the mGlu7 VFTD, was dose-dependently reduced by both XAP044 and

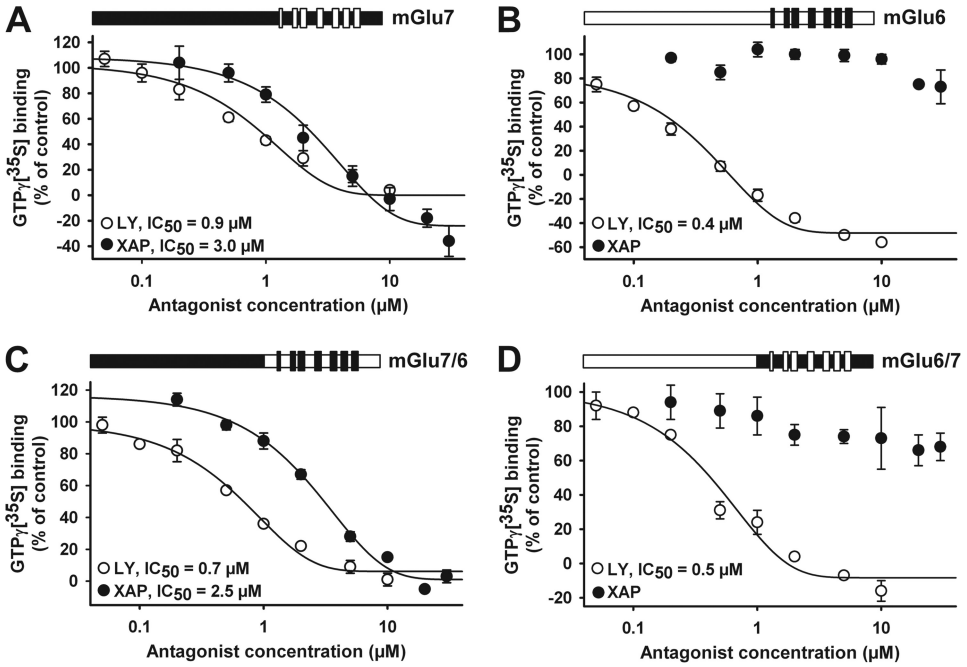

FIGURE 2. **XAP044 blocks G protein signaling via the VFTD of mGlu7.** *A–D,* concentration-response curves for XAP044 (*XAP*) and LY341495 (*LY*) against agonist (EC_{90})-stimulated [^{35}S]GTPγS (*GTPγ[35S]*) binding on membranes from CHO cells stably expressing either mGlu7 (*A*), mGlu6 (*B*), the chimeric receptors mGlu7/6 (*C*), or mGlu6/7 (*D*) as schematically depicted *above* each plot; the seven-transmembrane region is located to the *right* of each scheme and has been *highlighted* for better visibility. All data points represent the mean ± S.E. from at least three independent measurements ($n \geq 3$) normalized to the control stimulation of near-maximal agonist concentrations (*e.g.* 4 mM DL-AP4 in the case of mGlu7, set to 100%).

LY341495 with IC_{50} values of 2.5 and 0.7 μM, respectively (Fig. 2*C*). Only LY341495 reduced [^{35}S]GTPγS binding at the reciprocal mGlu6/7 chimeric receptor containing the mGlu6 VFTD (IC_{50} value of 0.5 μM; Fig. 2*D*). In conclusion, the antagonist action of XAP044 requires and is specific to the N-terminal extracellular VFTD of mGlu7.

Selectivity, Potency, and Profiling of XAP044 Using Different Second Messenger Assays—To extend selectivity characterization of XAP044 for mGlu7, its effects on [^{35}S]GTPγS binding were examined using CHO cell membranes stably expressing either human mGlu7b or mGlu2 (Fig. 3*A*). Increasing concentrations of XAP044 (up to 20 μM) completely blocked mGlu7 [^{35}S]GTPγS binding when stimulated with submaximal and near-maximal concentrations of DL-AP4 (EC_{20} = 100 μM and EC_{90} = 4000 μM); interestingly, 10 and 20 μM XAP044 result in [^{35}S]GTPγS binding values below baseline. A likely interpretation of this observation would be that mGlu7 expressed in our recombinant system has some constitutive activity, which can be blocked by XAP044. In contrast, XAP044 did not inhibit mGlu2 [^{35}S]GTPγS binding when stimulated with submaximal or near-maximal concentrations of L-glutamate (EC_{20} = 1 μM and EC_{90} = 50 μM; Fig. 3*A*). We also assessed inhibitory effects of XAP044 on forskolin-stimulated (10 μM) cAMP accumulation in CHO cells stably expressing either mGlu2, mGlu7, or $GABA_B$ receptors (Fig. 3*B*). XAP044 had no agonist-like effect on forskolin-stimulated cAMP accumulation in CHO cells expressing mGlu2, mGlu7, or $GABA_B$ receptors (values at ~110% of control stimulation obtained with 10 μM forskolin, Fig. 3*B*, *open symbols*). Following activation of these receptors using their respective agonists (50 μM L-glutamate/mGlu2; 50 μM GABA/$GABA_B$; 3 mM DL-AP4/mGlu7), cAMP accumulation remained at low levels for mGlu2 and $GABA_B$ (~30% of the levels obtained after stimulation with 10 μM forskolin; Fig. 3*B*), whereas increasing concentrations of XAP044 (up to 30 μM) on the mGlu7 cells reached cAMP levels comparable with those seen after stimulation with 10 μM forskolin (Fig. 3*B*, *filled circles*). In addition to the cAMP data shown in Fig. 3, we also conducted measurements at the cloned human mGlu8 subtype. Here, XAP044 showed weak antagonist activity with an IC_{50} value of 33 ± 9 μM (from n = 3 independent determinations). Taken together, these findings demonstrate the mGlu7-selective antagonist action of XAP044 in the cellular cAMP assay.

Next, we assessed the effects of increasing concentrations of XAP044 (up to 16 μM) on the intracellular Ca^{2+} response in the absence and presence of submaximal concentrations of L-glutamate (EC_{80} = 10 μM) or DL-AP4 (EC_{80} = 4000 μM) using mammalian cells stably expressing mGlu5a or the chimeric receptor mGlu7/5a (mGlu7 VFTD fused to mGlu5a transmembrane and intracellular region), respectively. XAP044 elicited strong inhibitory effects on the Ca^{2+} response via mGlu7/5a but had little effect on mGlu5a (40% inhibition at 16 μM, Fig. 3*C*). Concentration-response curves showed that XAP044 dose-dependently inhibited the DL-AP4-evoked (at EC_{80} = 4000 μM) Ca^{2+} response of CHO cells expressing the chimeric receptor mGlu7/5a (IC_{50} = 1.0 μM; Fig. 3*D*). Selectivity was further confirmed by showing that Ca^{2+} responses evoked by stimulating mGlu5a, V1a, or oxytocin receptors by their respective specific agonists was hardly affected by XAP044 (the IC_{50} for XAP044 was >20 μM in all cases; Fig. 3*D*). Taken together, these data clearly demonstrate that XAP044 shows selectivity for mGlu7 over several other GPCRs, independent of the assay used ([^{35}S]GTPγS binding, cAMP accumulation, and agonist-stimulated Ca^{2+} responses).

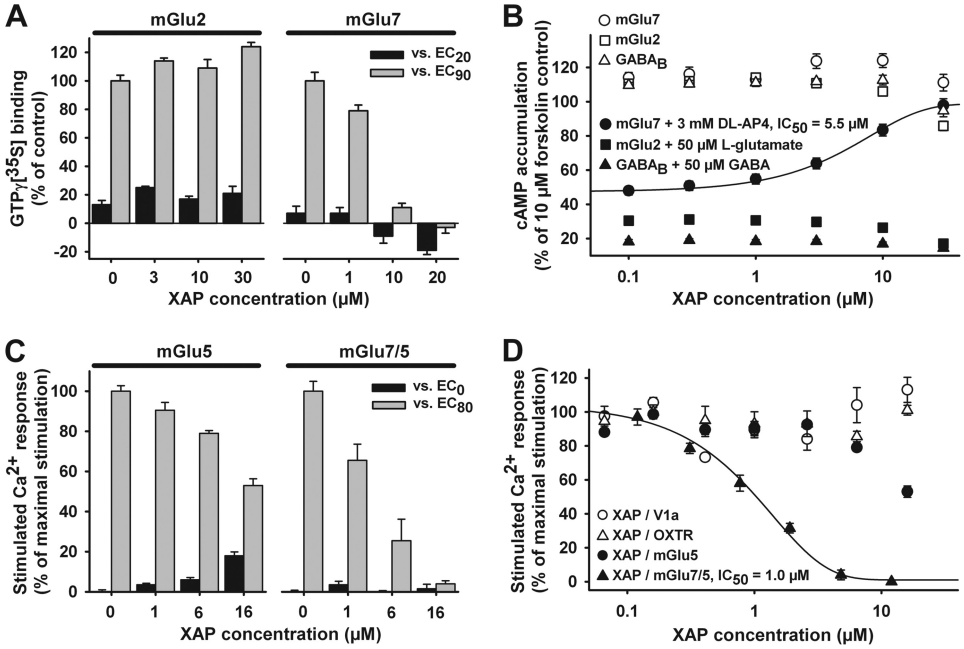

FIGURE 3. **Potency, mGlu7 selectivity, efficacy, and assay independence of XAP044.** *A,* effect of increasing concentrations of XAP044 (*XAP*) on [^{35}S]GTPγS (*GTPγ[^{35}S]*) binding in the presence of submaximal concentrations of L-glutamate (EC_{20} = 1 μM and EC_{90} = 50 μM) using membranes from CHO cells stably expressing mGlu2 or of DL-AP4 with mGlu7 membranes (EC_{20} = 100 μM and EC_{90} = 4000 μM). *B,* concentration-dependent effect of XAP044 on the inhibition of forskolin-stimulated cAMP accumulation in CHO cells stably expressing mGlu7, mGlu2, or $GABA_B$ in the absence (*open symbols*) or presence (*filled symbols*) of 3 mM DL-AP4, 50 μM L-glutamate, or 50 μM GABA, respectively; all data are normalized to the control stimulation of 10 μM forskolin (set to 100%). *C,* effect of increasing concentrations of XAP044 on the Ca^{2+} response of mammalian cells in the absence and presence of near-maximal concentrations of L-glutamate (EC_{80} = 10 μM) or DL-AP4 (EC_{80} = 4000 μM) using L cells stably expressing mGlu5a or CHO cells expressing the chimeric receptor mGlu7/5a, respectively. *D,* concentration-response curves for inhibition of agonist (EC_{80-90})-stimulated Ca^{2+} responses by XAP044 in stable cell lines expressing the V1a receptor, the oxytocin receptor, mGlu5a, or the chimeric receptor mGlu7/5a. All data represent the mean ± S.E. from at least three independent measurements ($n \geq 3$) normalized to the control stimulation of EC_{80-90} of the respective control agonists (set to 100%; *A, C,* and *D*) or 10 μM forskolin control (*B*).

XAP044 Antagonizes Thalamo-LA LTP via mGlu7—The mGlu7 antagonist XAP044 dose-dependently reduced the magnitude of LTP expressed at thalamo-LA synapses in mouse brain slices (Fig. 4*A*). Interestingly, the IC_{50} for this effect on LTP was below 0.1 μM, and maximum reduction of LTP occurred already at a concentration of 1 μM (Fig. 4*B*). Therefore, XAP044 seems 20-fold more potent at blocking thalamo-LA LTP in brain slices as compared with blocking signaling of recombinantly expressed mGlu7 receptors. To rule out that the effects of XAP044 on thalamo-LA LTP were nonspecific (*i.e.* independent of mGlu7), we tested whether XAP044 attenuates LTP also in brain slices of mice lacking mGlu7. XAP044 had no effect on the magnitude of thalamo-LA LTP expressed in brain slices from mGlu7 knock-out mice (unpaired *t* test, $p = 0.4$) but significantly reduced this LTP in wild type littermate slices (unpaired *t* test, $p = 0.03$), confirming that XAP044 attenuated LTP specifically via its actions on mGlu7 (Fig. 4, *C* and *D*). We also investigated whether the thalamo-LA LTP induced in our experiments was dependent on NMDA receptor activation as reported in rat slices (55, 56). The specific NMDA receptor antagonist CGP40116 significantly attenuated thalamo-LA LTP in slices from wild type mice and in slices from mice lacking mGlu7 to the same extent (Fig. 4, *E* and *F*). Thus, the LTP in wild type and mGlu7-deficient mice is NMDA receptor-dependent.

In Vivo Plasma and Brain Exposure of XAP044—Before conducting rodent behavioral studies, we determined exposure levels of XAP044 in plasma and brain. The i.p. administration of XAP044 in mice at 10 and 100 mg/kg yielded high plasma and brain concentrations 30 min after dosing. In both plasma and brain, XAP044 levels increased dose-proportionally from 2.8 to 33 μM (plasma) and from 1.6 to 13 μmol/kg (brain; mean of six mice for each dose). *In vitro* assessment of XAP044 binding to mouse and rat plasma protein as well as rat brain homogenate revealed high binding (>99%). Consequently, the free exposure of XAP044 in plasma and brain is assumed to be significantly lower as compared with the high total exposure that was detected.

Full Pharmacokinetic Profiles of XAP044 in Mice and Rats—In mice, XAP044 showed a high total blood clearance of 76 ml/min/kg and a very short apparent terminal half-life of 0.4 h (Table 1); the oral bioavailability was also low (17%), preventing XAP044 from being systemically or centrally available for a long time period after dose. Hence, the intraperitoneal route of administration was chosen for behavioral pharmacology in mice. Interestingly, the pharmacokinetic properties of XAP044 in rats were significantly better with a low plasma clearance of 12 ml/min/kg, a long apparent terminal half-life of 4.5 h and a good oral bioavailability (52%; see Table 1). Brain-to-blood or -plasma ratios in both species were very comparable ranging from 0.4 to 0.6 and independent of the compound's administration route.

In Vivo Activity of XAP044, Reduction of Physiological and Innate Anxiety and Inhibition of Depressive-like Behavior and Learned Fear—The role of mGlu7 in anxiety and stress behavior is well documented (10, 12, 14, 18, 22, 39). Several studies investigating mGlu7's role in emotional behavior indirectly suggested receptor blockade as a promising approach (9, 18). Therefore, we assessed the effects of the mGlu7 antagonist

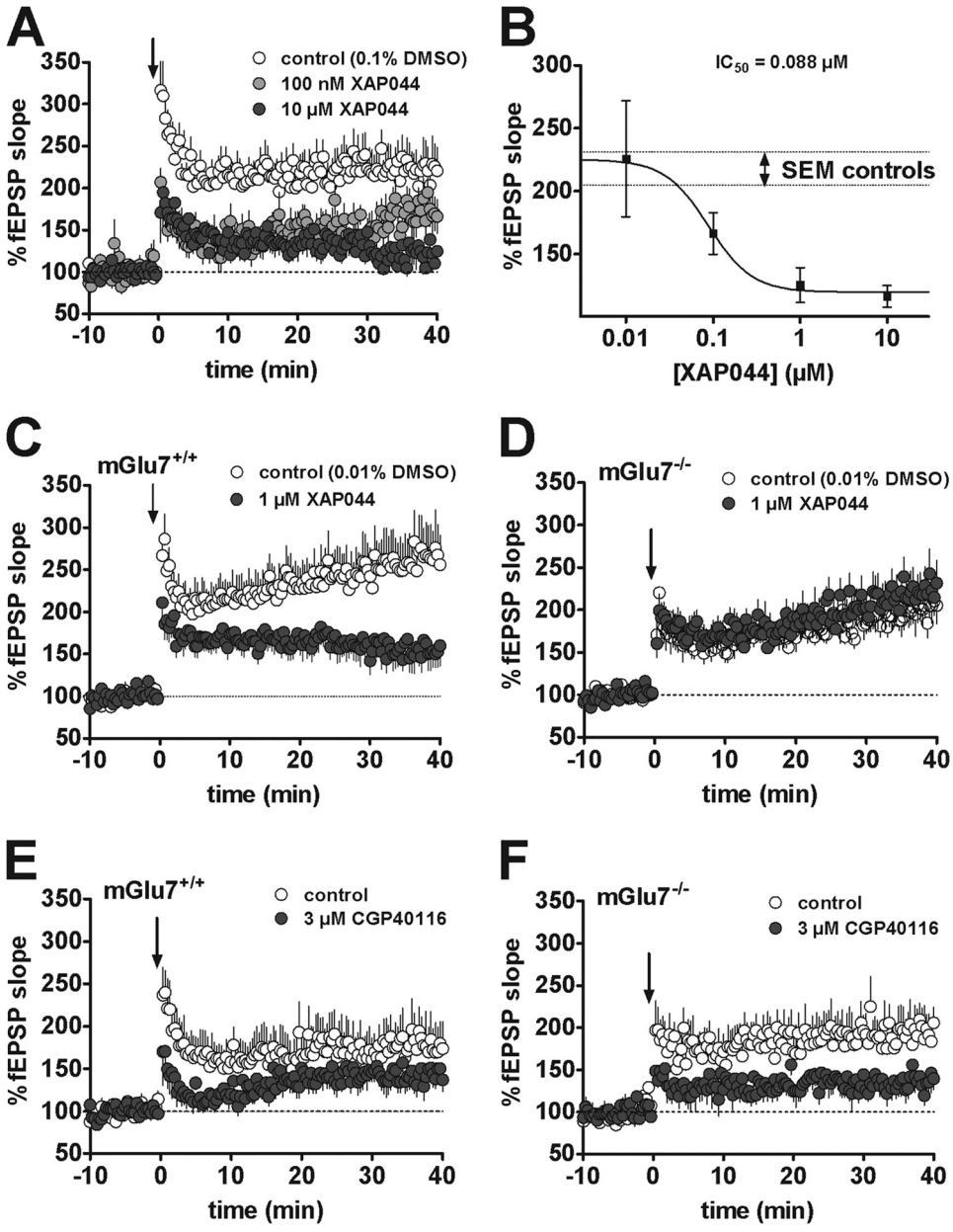

FIGURE 4. **XAP044 attenuates thalamo-lateral amygdala LTP in an mGlu7-dependent manner.** fEPSP were recorded in the LA and evoked by stimulation of thalamic inputs. *A,* time course of thalamo-LA LTP induced by five 1-s trains of 100 Hz stimuli (at time 0 min, *arrow*) in the absence ($n = 8$, DMSO control) or presence of 100 nM ($n = 7$) and 10 µM ($n = 9$) XAP044 (*XAP*) after 10-min stable baseline in brain slices of wild type mice. *B,* fEPSP slope 30–40 min after induction of LTP in the presence of 0.01 µM ($n = 6$), 0.1 µM ($n = 7$), 1 µM ($n = 7$), and 10 µM ($n = 9$) of XAP044. *C* and *D,* time course of thalamo-LA LTP induced by five 1-s trains of 100 Hz stimuli (at time 0 min, *arrow*) in the absence ($n = 9$, DMSO control) or presence of 1 µM XAP044 ($n = 11$–13) after 10-min stable baseline in brain slices of wild type mice (mGlu7$^{+/+}$; *C*) and mGlu7-deficient mice (mGlu7$^{-/-}$; *D*). *E* and *F,* time course of thalamo-LA LTP induced by five 1-s trains of 100 Hz stimuli (at time 0 min, *arrow*) in the absence ($n = 7$–8, DMSO control) or presence of 3 µM CGP40116 ($n = 8$–11) after 10-min stable baseline in brain slices of wild type mice (mGlu7$^{+/+}$; *E*) and mGlu7-deficient mice (mGlu7$^{-/-}$; *F*). All data represent the mean ± S.E. normalized to the average baseline for each slice (set to 100%).

XAP044 in a battery of behavioral tests, including SIH, TST, EPM, and Pavlovian fear conditioning in mice.

SIH Test—Treatment with the orthosteric-like mGlu7 antagonist XAP044 dose-dependently attenuated the stress-induced rise in rectal body temperature ($H(4) = 20.1, p < 0.001$; Fig. 5*A*). The post hoc analysis revealed no significant effect of 10 mg/kg of XAP044 ($p > 0.05$), whereas 30 mg/kg ($p = 0.009$) as well as 60 mg/kg ($p = 0.006$) of XAP044 significantly attenuated the stress-induced rise in rectal temperature compared with vehicle-treated animals. As expected, SIH was also reduced by the benzodiazepine-anxiolytic chlorodiazepoxide (10 mg/kg, $p < 0.001$; Fig. 5*A*), which was used as a positive control. XAP044 did not show any significant effect on basal body temperature at any of the tested doses ($p > 0.05$ in all cases; data not shown).

TST—XAP044 treatment also decreased immobility in the TST ($H(3) = 32.2, p < 0.001$; Fig. 5*B*). Both 10 mg/kg ($p = 0.01$) and 60 mg/kg ($p = 0.001$) of XAP044-injected intraperitoneally significantly reduced the time the mice spent immobile compared with vehicle-treated animals. Injection of the tricyclic antidepressant imipramine (20 mg/kg; $p < 0.001$), used as pos-

TABLE 1

Pharmacokinetic profiles of XAP044 in mice and rats

The absorption and disposition parameters were estimated by a noncompartmental analysis of the mean blood concentration ($n = 3$) *versus* time profile after p.o. and i.v. administration. The apparent terminal phase rate constant was determined by choosing the last three data points from the log-linear regression of the blood concentrations *versus* time curve and was used for the extrapolation of the area under the curve (AUC) to infinity. The absolute oral bioavailability (BAV) was calculated by dividing the dose-normalized (d.n.) AUC after p.o. administration by the respective AUC after i.v. administration assuming linear pharmacokinetics between the intravenous and oral doses.

Parameter/species	Mouse	Rat
Doses (i.v./p.o. (mg/kg))	1.0/3.0	3.0/10.0
Matrix	Blood	Plasma
Strain, gender	C57BL/6, male	Sprague-Dawley, male
Cl (ml/min/kg)	76	12
V_{ss} (liter/kg)	0.9	3.0
MRT (h)	0.2	4.3
$t_{½}$ (h)	0.4	4.5
AUC i.v., d.n. (nmol·h)	576	3691
AUC p.o., d.n. (nmol·h)	95	1907
BAV (%)	17	52
C_{max} d.n. (nmol)	55	140
t_{max} (h)	0.3	8
Brain/blood (mouse) or brain/plasma (rat) ratio	0.4–0.6	0.4–0.6

itive control, also reduced the immobility time compared with the vehicle group.

EPM Test—Moreover, XAP044 treatment decreased innate anxiety-related behavior in the EPM ($H(3) = 19.4$, $p < 0.001$; Fig. 5*C*). At a dose of 60 mg/kg, the intraperitoneally injected XAP044 significantly increased the ratio of open/total arm entries on the EPM ($p = 0.006$) compared with vehicle-treated mice, indicative of a decrease in anxiety-related behavior (Fig. 5*C*). The same effect was seen in mice treated with the benzodiazepine diazepam (1 mg/kg; $p < 0.001$; Fig. 5 *C*), used as positive control. Importantly, the number of total arm entries as an indicator of locomotor activity (Fig. 5*D*) was neither affected by XAP044 nor by diazepam treatment ($H(3) = 3.2$, $p = 0.361$; Fig. 5*D*).

Pavlovian Fear Conditioning—Freezing of the mice during the fear conditioning session on day 1 was found to be significantly affected by treatment ($F_{3,35} = 16.992$, $p \leq 0.001$). Furthermore, the level of freezing increased across CS-US pairings ($F_{5,175} = 154.599$, $p \leq 0.001$). Also, XAP044 injected intraperitoneally at a dose of 60 mg/kg resulted in less freezing during the fear acquisition session compared with the vehicle group, which was statistically significant when CS-US pairings were presented for the third time ($p = 0.030$; Fig. 5*E*) and a trend was observed at the fifth CS-US pairing ($p = 0.077$; Fig. 5*E*). This is indicative of delayed short term fear acquisition by XAP044. As a positive control for delayed fear acquisition, the allosteric mGlu5 antagonist MPEP was used (30 mg/kg), which resulted in a significant reduction of the freezing response across all trials ($p \leq 0.032$ for all pairings). Additionally, fear expression was assessed on the 2nd day. However, neither XAP044 nor MPEP had any effect on the freezing response compared with vehicle-treated animals at CS presentations ($F_{3,35} = 1.040$, $p = 0.387$; Fig. 5*F*). The effect of XAP044 to delay short term fear acquisition *in vivo* corresponds well with XAP044's mGlu7-dependent inhibition of LTP in the lateral amygdala, an assay that is considered an *in vitro* electrophysiological correlate of fear learning.

DISCUSSION

In these studies, we present XAP044, the first mGlu7-selective full antagonist that blocks the receptor's signaling pathways via binding to the large extracellular VFTD region of this class C GPCR. Thus, XAP044 presumably acts via a novel site compared with known selective ligands. XAP044 selectively blocks LTP in the lateral amygdala of wild type but not of mGlu7-deficient mice, further substantiating a role for mGlu7 in the cellular physiology of the fear and emotion circuitry. XAP044 is systemically active and demonstrates wide spectrum antistress, antidepressant-, and anxiolytic-like efficacy *in vivo*. Pharmacological blockade of mGlu7 thus is a very promising mechanism for future treatment of various disorders of emotion in man.

XAP044 elicited full antagonist action at mGlu7 that is comparable with classical L-glutamate-site blockers such as magnesium/pyridoxal-5′-phosphate glutamate (MPPG) or α-cyclopropyl-4-phosphonophenylglycine (CPPG), which, unlike XAP044, do not discriminate between the four group III mGlu subtypes (Ref. 7 and references therein). Our data with chimeric receptors strongly suggest the localization of a novel pharmacological site for XAP044-type antagonists within the VFTD region of mGlu7. We also showed that XAP044 lacks activity at other G_i-coupled mGlu and GABA receptors when expressed in identical host cells. Our functional studies provide strong support for a direct interaction of XAP044 with mGlu7 because its mGlu7-dependent and -selective antagonism is seen in the [^{35}S]GTPγS binding assay, as well as in two different second messenger assays (cAMP and Ca^{2+}; Figs. 1–3). Furthermore, we specifically showed that XAP044 blocks [^{35}S]GTPγS binding stimulated by the orthosteric agonist DL-AP4, whereas XAP044 did not inhibit [^{35}S]GTPγS binding stimulated by the mGlu7 allosteric agonist AMN082. This selective mode of action of XAP044 differs from the mGlu7 NAM MMPIP, which also inhibits the actions of AMN082 (28, 29). Therefore, independent lines of evidence suggest that XAP044 is a selective and orthosteric-like antagonist that acts at a specific binding site located within the VFTD of mGlu7.

Previously, the synthesis of mGlu7 subtype-selective antagonists that act via the receptor's VFTD has been elusive, presumably because orthosteric receptor activation was mostly achieved by compounds with an α-amino acid moiety and a distal ionizable group (*e.g.* an ω-phosphono residue), and such

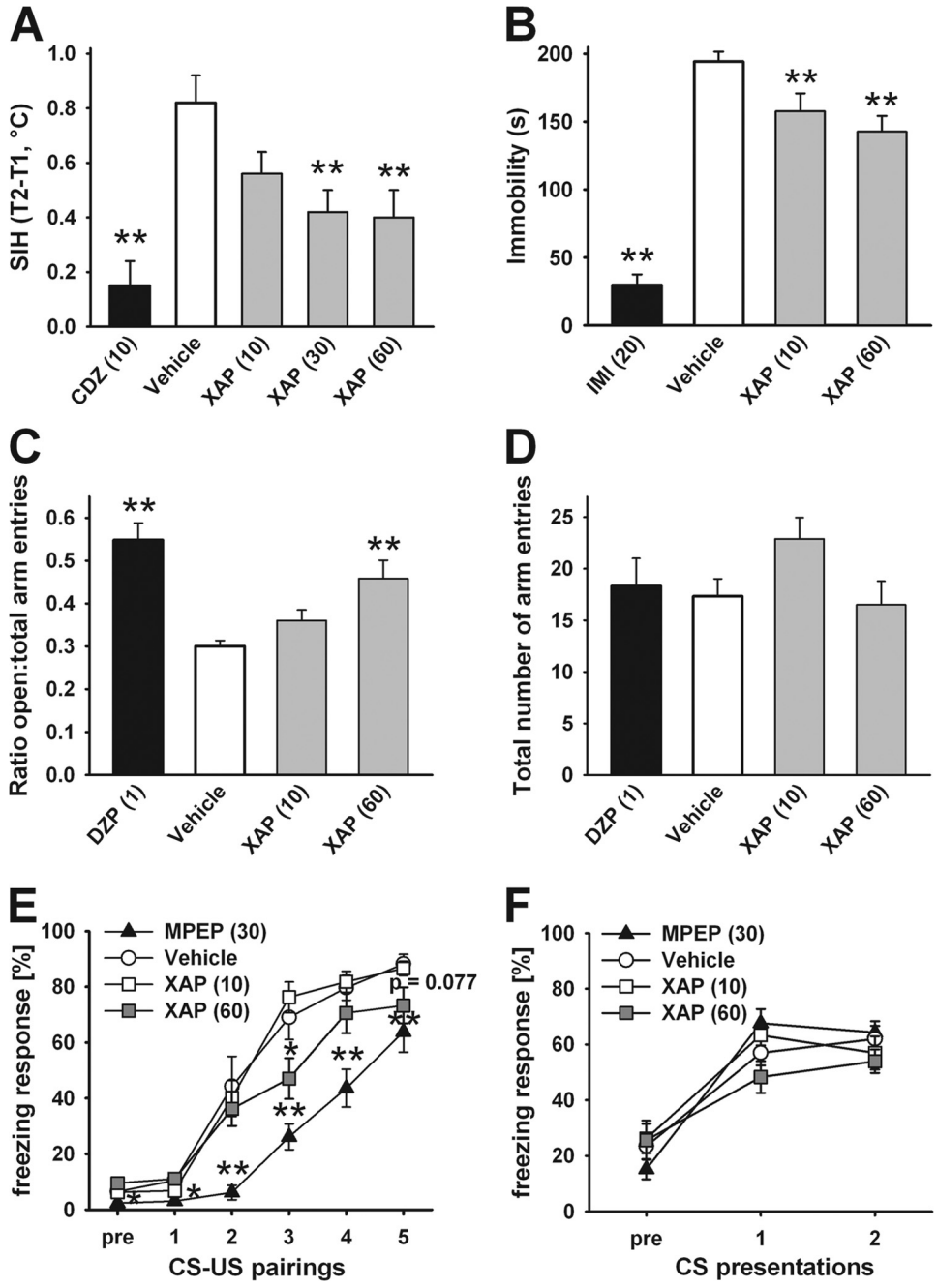

FIGURE 5. **XAP044 relieves physiological and innate anxiety and depressive-like behavior and reduces freezing during the acquisition session of fear conditioning.** *A,* SIH (*t*2–*t*1 in °C) 30 min after i.p. injection of chlorodiazepoxide (10 mg/kg; positive control), vehicle, or XAP044 (*XAP*) (10, 30, and 60 mg/kg) in mice. *B,* immobility time (second) in the tail suspension test 30 min after i.p. injection of imipramine (20 mg/kg; positive control), vehicle, or XAP044 (10 and 60 mg/kg) in mice. *C* and *D,* ratio open/total arm entries (*C*) and total number of arm entries (*D*) on the elevated plus-maze 30 min after intraperitoneal injection of diazepam (1 mg/kg; positive control), vehicle, or XAP044 (10 and 60 mg/kg) in mice. *E* and *F,* freezing responses (% of time during conditioned stimulus (*CS*) presentation) during the acquisition of cued fear (*E*) starting 30 min after intraperitoneal injection of either MPEP (30 mg/kg; positive control), vehicle, or XAP044 (10 and 60 mg/kg) and expression test on learned fear 1 day after the conditioning session (*F*) in mice. All data represent the mean ± S.E. *, $p < 0.05$; **, $p < 0.01$ *versus* vehicle group, Kruskal-Wallis ANOVA followed by a post hoc Dunnett´s test (*A*--*D*) or repeated measures ANOVA followed by a post hoc least significant difference test (*E* and *F*); $n = 8$–14 per treatment group. *CDZ,* chlorodiazepoxide; *IMI,* imipramine; *DZP*, diazepam; *US*, unconditioned stimulus.

molecules had no preference for mGlu7 over other group III receptors and are often too hydrophilic to cross biological membranes, in particular the blood-brain barrier. Group III antagonists were mostly obtained by turning such agonists into antagonists via replacing the α-proton of the amino acid agonists by a bulky substituent that prevents closing of the VFTD lobes (*e.g.* MPPG, CPPG, (*S*)-2-amino-2-methyl-4-phosphonobutanoic acid (MAP4), and (1*R*,3*R*,4*S*)-1-aminocyclopentane-1,3,4-tricarboxylic acid (ACPT-II) (6, 7)). Like their group III agonist counterparts, these kind of antagonists lack mGlu7 selectivity and reliable systemic activity. In contrast, our novel orthosteric-like antagonist XAP044 is in structural terms completely unrelated to amino acids. Its physicochemical properties allow peripheral administration and permit significant penetration of the blood-brain barrier, resulting in substantial blood and brain exposures. Furthermore, XAP044 is receptor

subtype-selective, showing only moderate inhibition of mGlu5 and mGlu8 at the highest concentrations tested ($IC_{50} > 20\ \mu M$ and $> 30\ \mu M$, respectively; see under "Results"), and no activity at mGlu4, mGlu6, $GABA_B$, oxytocin, and V1a receptors. The new mode-of-action of XAP044 thus paves the way for new and attractive drug development opportunities targeting mGlu7 and other VFTD-containing class C GPCRs that are of therapeutic interest.

Thalamo-LA LTP requires both mGlu5 and NMDA receptors (55, 56). As the reduction of LTP by XAP044 at 1 μM was completely abolished in mice lacking mGlu7, it is highly unlikely that the weak antagonistic effects of XAP044 on mGlu5 could be contributing to the reduction of LTP as mGlu5-dependent effects would remain apparent in the knock-outs. XAP044 attenuated the initial facilitation following the high frequency stimulation and LTP. Likewise, both post-tetanic facilitation and LTP are reduced in mGlu7-deficient mice (see also Ref. 14), and in these mice there was no additional effect of XAP044 on either parameter (see Fig. 4). Thus, both post-tetanic potentiation and the resulting LTP of thalamo-LA EPSPs are modulated by mGlu7. In contrast, normal low frequency transmission in LA is modified by mGlu8 and not by mGlu7 (14, 23). We also verified that the thalamo-LA LTP in mice has similar NMDA dependence than LTP in rats (see Fig. 4). Rather surprisingly, XAP044 was significantly more potent in blocking thalamo-LA LTP than it was at blocking mGlu7 in the recombinant receptor assays. The half-maximal blockade of LTP occurred at 88 nM, whereas IC_{50} values of 2–5 μM were measured in the assays using recombinant cells. At the present time, it remains unclear why these differences in apparent potency exist. One possibility is that endogenous proteins, such as receptor activity-modifying proteins, interact with mGlu7 in neurons conferring higher affinity for the antagonist than is measured in recombinant systems where such proteins may be absent (57). Alternatively, mGlu7 may influence synaptic plasticity in the amygdala via signaling pathway(s) distinct from those of G_i used in the recombinant assays, and the apparent potency of XAP044 for these two pathways may differ. Such ligand bias is well documented for GPCRs, for instance the affinity of the κ-opioid receptor for agonists may change 18-fold depending on which G protein it is coupled (58). Further studies are required to understand whether either of these possibilities may be the case for XAP044 and mGlu7.

mGlu7 has been shown to play a critical role in amygdala plasticity (14, 22) and at dentate granule cell synapses contacting CA3 interneurons (59–61). However, the dearth of specific pharmacological tools has hampered further progress in understanding the physiological roles of mGlu7 and potential therapeutic applications. The nonselective agonist L-AP4, which also interacts with other group III mGlu subtypes, and AMN082, an allosteric agonist but at the same time a strong inducer of mGlu7 internalization, were the main tools available (24, 39, 62). More recently, different mGlu7-selective NAMs have been reported (26, 29), which blocked mGlu7 selectively in recombinant cells. However, a stringent assessment of their mGlu7-dependent action in native brain tissues and assays is still missing.

The data of our *in vivo* experiments with XAP044 are consistent with published data on the behavior of mGlu7-deficient mice. These mice showed reduced anxiety- and depression-like behavior in several experimental paradigms, such as the SIH test, the marble-burying test, the forced swim test, the TST, the light-dark box, the staircase test, and the EPM test (11, 12). mGlu7-deficient mice also express a strong general deficit in conditioned fear, whereas mGlu8-deficient mice show a specific but dramatic reduction in contextual fear (14, 23). Systemic application of XAP044 had very similar behavioral effects as mGlu7 deficiency, a dose-dependent reduction of SIH, slightly reduced immobility in the TST, an increased ratio of open/total arm entries in the EPM test, and less freezing during the acquisition session of Pavlovian fear conditioning (Fig. 5). All of this is not only consistent with the phenotype of mGlu7-deficient mice but also with mGlu7 siRNA-mediated knockdown studies (11–15, 18, 22, 63). The main difference between the effects of XAP044 and mGlu7-deficient mice was the compound's low efficacy in TST (Fig. 5) and in the forced swim test (FST, $n = 3$ independent measurements with no significant reduction in immobility). Interestingly, the effects of the mGlu7 antagonist XAP044 are, at least in part, similar to those previously reported for the allosteric agonist AMN082 (13, 21). However, as discussed above and earlier (14, 22), this apparent discrepancy can potentially be explained by the rapid AMN082-induced mGlu7 internalization or effects of active metabolites (see Introduction). It is worth noting that despite widespread efficacy of XAP044 in tests of anxiety and stress, the magnitudes of such effects were less than those of either benzodiazepines, the mGlu5 antagonist MPEP, or mGlu7-deficient mice. This difference in efficacy might be explained by the low concentration of free compared with total XAP044 in brain and plasma (see PK studies above), a drawback of XAP044 that can likely be overcome with future chemical derivatives. Nonetheless, our results with XAP044 further substantiate an important role for mGlu7 in the behavioral physiology of stress, fear, and anxiety.

In conclusion, we have identified an mGlu7-selective antagonist, XAP044, that acts via a binding site within the VFTD region of this class C GPCR and can serve as an invaluable tool for further unraveling the physiological roles of mGlu7. Moreover, XAP044's novel molecular mode of pharmacological blockade carries significant application potential in psychiatry, *e.g.* in anxiety, mood, and somatic stress-related disorders. XAP044 blocks mGlu7 signaling via the VFTD, whose three-dimensional structure is already known (32, 33). Modeling the interaction of XAP044 within the VFTD of mGlu7, followed by computer-assisted drug design, will facilitate future drug development.

Acknowledgments—We thank Drs. G. Bilbe and K. McAllister for giving continuous support and for critical and very helpful discussions. We also thank K. Fizia, S. Felice, P. Martin, and C. Mattes for excellent technical assistance.

REFERENCES

1. Bhattacharya, S., Lam, A. R., Li, H., Balaraman, G., Niesen, M. J., and Vaidehi, N. (2013) Critical analysis of the successes and failures of homol-

ogy models of G protein-coupled receptors. *Proteins* **81,** 729–739
2. Bockaert, J., and Pin, J. P. (1999) Molecular tinkering of G protein-coupled receptors: An evolutionary success. *EMBO J.* **18,** 1723–1729
3. Foord, S. M., Bonner, T. I., Neubig, R. R., Rosser, E. M., Pin, J. P., Davenport, A. P., Spedding, M., and Harmar, A. J. (2005) International Union of Pharmacology. XLVI. G protein-coupled receptor list. *Pharmacol. Rev.* **57,** 279–288
4. Pin, J. P., Galvez, T., and Prézeau, L. (2003) Evolution, structure, and activation mechanism of family 3/C G-protein-coupled receptors. *Pharmacol. Ther.* **98,** 325–354
5. Wauson, E. M., Lorente-Rodríguez, A., and Cobb, M. H. (2013) Minireview: nutrient sensing by G protein-coupled receptors. *Mol. Endocrinol.* **27,** 1188–1197
6. Bessis, A. S., Rondard, P., Gaven, F., Brabet, I., Triballeau, N., Prezeau, L., Acher, F., and Pin, J. P. (2002) Closure of the Venus flytrap module of mGlu8 receptor and the activation process: Insights from mutations converting antagonists into agonists. *Proc. Natl. Acad. Sci. U.S.A.* **99,** 11097–11102
7. Flor, P. J., and Acher, F. C. (2012) Orthosteric *versus* allosteric GPCR activation: The great challenge of group-III mGluRs. *Biochem. Pharmacol.* **84,** 414–424
8. Flor, P. J., Van Der Putten, H., Rüegg, D., Lukic, S., Leonhardt, T., Bence, M., Sansig, G., Knöpfel, T., and Kuhn, R. (1997) A novel splice variant of a metabotropic glutamate receptor, human mGluR7b. *Neuropharmacology* **36,** 153–159
9. O'Connor, R. M., Finger, B. C., Flor, P. J., and Cryan, J. F. (2010) Metabotropic glutamate receptor 7: At the interface of cognition and emotion. *Eur. J. Pharmacol.* **639,** 123–131
10. Masugi, M., Yokoi, M., Shigemoto, R., Muguruma, K., Watanabe, Y., Sansig, G., van der Putten, H., and Nakanishi, S. (1999) Metabotropic glutamate receptor subtype 7 ablation causes deficit in fear response and conditioned taste aversion. *J. Neurosci.* **19,** 955–963
11. Callaerts-Vegh, Z., Beckers, T., Ball, S. M., Baeyens, F., Callaerts, P. F., Cryan, J. F., Molnar, E., and D'Hooge, R. (2006) Concomitant deficits in working memory and fear extinction are functionally dissociated from reduced anxiety in metabotropic glutamate receptor 7-deficient mice. *J. Neurosci.* **26,** 6573–6582
12. Cryan, J. F., Kelly, P. H., Neijt, H. C., Sansig, G., Flor, P. J., and van Der Putten, H. (2003) Antidepressant and anxiolytic-like effects in mice lacking the group III metabotropic glutamate receptor mGluR7. *Eur. J. Neurosci.* **17,** 2409–2417
13. Stachowicz, K., Brański, P., Kłak, K., van der Putten, H., Cryan, J. F., Flor, P. J., and Andrzej, P. (2008) Selective activation of metabotropic G-protein-coupled glutamate 7 receptor elicits anxiolytic-like effects in mice by modulating GABAergic neurotransmission. *Behav. Pharmacol.* **19,** 597–603
14. Fendt, M., Imobersteg, S., Peterlik, D., Chaperon, F., Mattes, C., Wittmann, C., Olpe, H. R., Mosbacher, J., Vranesic, I., van der Putten, H., McAllister, K. H., Flor, P. J., and Gee, C. E. (2013) Differential roles of mGlu7 and mGlu8 in amygdala-dependent behavior and physiology. *Neuropharmacology* **72,** 215–223
15. Mitsukawa, K., Mombereau, C., Lötscher, E., Uzunov, D. P., van der Putten, H., Flor, P. J., and Cryan, J. F. (2006) Metabotropic glutamate receptor subtype 7 ablation causes dysregulation of the HPA axis and increases hippocampal BDNF protein levels: Implications for stress-related psychiatric disorders. *Neuropsychopharmacology* **31,** 1112–1122
16. Martín, R., Durroux, T., Ciruela, F., Torres, M., Pin, J. P., and Sánchez-Prieto, J. (2010) The metabotropic glutamate receptor mGlu7 activates phospholipase C, translocates munc-13-1 protein, and potentiates glutamate release at cerebrocortical nerve terminals. *J. Biol. Chem.* **285,** 17907–17917
17. Schoepp, D. D. (2001) Unveiling the functions of presynaptic metabotropic glutamate receptors in the central nervous system. *J. Pharmacol. Exp. Ther.* **299,** 12–20
18. O'Connor, R. M., Thakker, D. R., Schmutz, M., van der Putten, H., Hoyer, D., Flor, P. J., and Cryan, J. F. (2013) Adult siRNA-induced knockdown of mGlu7 receptors reduces anxiety in the mouse. *Neuropharmacology* **72,** 66–73
19. Nicoletti, F., Bockaert, J., Collingridge, G. L., Conn, P. J., Ferraguti, F., Schoepp, D. D., Wroblewski, J. T., and Pin, J. P. (2011) Metabotropic glutamate receptors: From the workbench to the bedside. *Neuropharmacology* **60,** 1017–1041
20. Palazzo, E., Fu, Y., Ji, G., Maione, S., and Neugebauer, V. (2008) Group III mGluR7 and mGluR8 in the amygdala differentially modulate nocifensive and affective pain behaviors. *Neuropharmacology* **55,** 537–545
21. Palucha, A., Klak, K., Branski, P., van der Putten, H., Flor, P. J., and Pilc, A. (2007) Activation of the mGlu7 receptor elicits antidepressant-like effects in mice. *Psychopharmacology* **194,** 555–562
22. Fendt, M., Schmid, S., Thakker, D. R., Jacobson, L. H., Yamamoto, R., Mitsukawa, K., Maier, R., Natt, F., Hüsken, D., Kelly, P. H., McAllister, K. H., Hoyer, D., van der Putten, H., Cryan, J. F., and Flor, P. J. (2008) mGluR7 facilitates extinction of aversive memories and controls amygdala plasticity. *Mol. Psychiatry* **13,** 970–979
23. Dobi, A., Sartori, S. B., Busti, D., Van der Putten, H., Singewald, N., Shigemoto, R., and Ferraguti, F. (2013) Neural substrates for the distinct effects of presynaptic group III metabotropic glutamate receptors on extinction of contextual fear conditioning in mice. *Neuropharmacology* **66,** 274–289
24. Pelkey, K. A., Yuan, X., Lavezzari, G., Roche, K. W., and McBain, C. J. (2007) mGluR7 undergoes rapid internalization in response to activation by the allosteric agonist AMN082. *Neuropharmacology* **52,** 108–117
25. Sukoff Rizzo, S. J., Leonard, S. K., Gilbert, A., Dollings, P., Smith, D. L., Zhang, M. Y., Di, L., Platt, B. J., Neal, S., Dwyer, J. M., Bender, C. N., Zhang, J., Lock, T., Kowal, D., Kramer, A., Randall, A., Huselton, C., Vishwanathan, K., Tse, S. Y., Butera, J., Ring, R. H., Rosenzweig-Lipson, S., Hughes, Z. A., and Dunlop, J. (2011) The metabotropic glutamate receptor 7 allosteric modulator AMN082: A monoaminergic agent in disguise? *J. Pharmacol. Exp. Ther.* **338,** 345–352
26. Kalinichev, M., Rouillier, M., Girard, F., Royer-Urios, I., Bournique, B., Finn, T., Charvin, D., Campo, B., Le Poul, E., Mutel, V., Poli, S., Neale, S. A., Salt, T. E., and Lütjens, R. (2013) ADX71743, a potent and selective negative allosteric modulator of metabotropic glutamate receptor 7: *In vitro* and *in vivo* characterization. *J. Pharmacol. Exp. Ther.* **344,** 624–636
27. Hikichi, H., Murai, T., Okuda, S., Maehara, S., Satow, A., Ise, S., Nishino, M., Suzuki, G., Takehana, H., Hata, M., and Ohta, H. (2010) Effects of a novel metabotropic glutamate receptor 7 negative allosteric modulator, 6-(4-methoxyphenyl)-5-methyl-3-pyridin-4-ylisoxazonolo[4,5-c]pyridin-4(5*H*)-one (MMPIP), on the central nervous system in rodents. *Eur. J. Pharmacol.* **639,** 106–114
28. Nakamura, M., Kurihara, H., Suzuki, G., Mitsuya, M., Ohkubo, M., and Ohta, H. (2010) Isoxazolopyridone derivatives as allosteric metabotropic glutamate receptor 7 antagonists. *Bioorg. Med. Chem. Lett.* **20,** 726–729
29. Suzuki, G., Tsukamoto, N., Fushiki, H., Kawagishi, A., Nakamura, M., Kurihara, H., Mitsuya, M., Ohkubo, M., and Ohta, H. (2007) *In vitro* pharmacological characterization of novel isoxazolopyridone derivatives as allosteric metabotropic glutamate receptor 7 antagonists. *J. Pharmacol. Exp. Ther.* **323,** 147–156
30. Niswender, C. M., Johnson, K. A., Miller, N. R., Ayala, J. E., Luo, Q., Williams, R., Saleh, S., Orton, D., Weaver, C. D., and Conn, P. J. (2010) Context-dependent pharmacology exhibited by negative allosteric modulators of metabotropic glutamate receptor 7. *Mol. Pharmacol.* **77,** 459–468
31. Kunishima, N., Shimada, Y., Tsuji, Y., Sato, T., Yamamoto, M., Kumasaka, T., Nakanishi, S., Jingami, H., and Morikawa, K. (2000) Structural basis of glutamate recognition by a dimeric metabotropic glutamate receptor. *Nature* **407,** 971–977
32. Muto, T., Tsuchiya, D., Morikawa, K., and Jingami, H. (2007) Expression, purification, crystallization and preliminary x-ray analysis of the ligand-binding domain of metabotropic glutamate receptor 7. *Acta Crystallogr. Sect. F Struct. Biol. Cryst. Commun.* **63,** 627–630
33. Muto, T., Tsuchiya, D., Morikawa, K., and Jingami, H. (2007) Structures of the extracellular regions of the group II/III metabotropic glutamate receptors. *Proc. Natl. Acad. Sci. U.S.A.* **104,** 3759–3764
34. Tsuchiya, D., Kunishima, N., Kamiya, N., Jingami, H., and Morikawa, K. (2002) Structural views of the ligand-binding cores of a metabotropic glutamate receptor complexed with an antagonist and both glutamate and Gd^{3+}. *Proc. Natl. Acad. Sci. U.S.A.* **99,** 2660–2665
35. Topiol, S., Sabio, M., and Uberti, M. (2011) Exploration of structure-based

drug design opportunities for mGluRs. *Neuropharmacology* **60,** 93–101
36. Flor, P. J., Lukic, S., Rüegg, D., Leonhardt, T., Knöpfel, T., and Kuhn, R. (1995) Molecular cloning, functional expression and pharmacological characterization of the human metabotropic glutamate receptor type 4. *Neuropharmacology* **34,** 149–155
37. Gasparini, F., Bruno, V., Battaglia, G., Lukic, S., Leonhardt, T., Inderbitzin, W., Laurie, D., Sommer, B., Varney, M. A., Hess, S. D., Johnson, E. C., Kuhn, R., Urwyler, S., Sauer, D., Portet, C., Schmutz, M., Nicoletti, F., and Flor, P. J. (1999) (*R,S*)-4-Phosphonophenylglycine, a potent and selective group III metabotropic glutamate receptor agonist, is anticonvulsive and neuroprotective *in vivo*. *J. Pharmacol. Exp. Ther.* **289,** 1678–1687
38. Gasparini, F., Lingenhöhl, K., Stoehr, N., Flor, P. J., Heinrich, M., Vranesic, I., Biollaz, M., Allgeier, H., Heckendorn, R., Urwyler, S., Varney, M. A., Johnson, E. C., Hess, S. D., Rao, S. P., Sacaan, A. I., Santori, E. M., Veliçelebi, G., and Kuhn, R. (1999) 2-Methyl-6-(phenylethynyl)-pyridine (MPEP), a potent, selective and systemically active mGlu5 receptor antagonist. *Neuropharmacology* **38,** 1493–1503
39. Mitsukawa, K., Yamamoto, R., Ofner, S., Nozulak, J., Pescott, O., Lukic, S., Stoehr, N., Mombereau, C., Kuhn, R., McAllister, K. H., van der Putten, H., Cryan, J. F., and Flor, P. J. (2005) A selective metabotropic glutamate receptor 7 agonist: Activation of receptor signaling via an allosteric site modulates stress parameters *in vivo*. *Proc. Natl. Acad. Sci. U.S.A.* **102,** 18712–18717
40. Weng, K., Lu, C., Daggett, L. P., Kuhn, R., Flor, P. J., Johnson, E. C., and Robinson, P. R. (1997) Functional coupling of a human retinal metabotropic glutamate receptor (hmGluR6) to bovine rod transducin and rat G_o in an *in vitro* reconstitution system. *J. Biol. Chem.* **272,** 33100–33104
41. Tones, M. A., Bendali, N., Flor, P. J., Knöpfel, T., and Kuhn, R. (1995) The agonist selectivity of a class III metabotropic glutamate receptor, human mGluR4a, is determined by the N-terminal extracellular domain. *Neuroreport* **7,** 117–120
42. Maj, M., Bruno, V., Dragic, Z., Yamamoto, R., Battaglia, G., Inderbitzin, W., Stoehr, N., Stein, T., Gasparini, F., Vranesic, I., Kuhn, R., Nicoletti, F., and Flor, P. J. (2003) (−)-PHCCC, a positive allosteric modulator of mGluR4: characterization, mechanism of action, and neuroprotection. *Neuropharmacology* **45,** 895–906
43. Lin, F. F., Varney, M., Sacaan, A. I., Jachec, C., Daggett, L. P., Rao, S., Flor, P., Kuhn, R., Kerner, J. A., Standaert, D., Young, A. B., and Veliçelebi, G. (1997) Cloning and stable expression of the mGluR1b subtype of human metabotropic receptors and pharmacological comparison with the mGluR5a subtype. *Neuropharmacology* **36,** 917–931
44. Litschig, S., Gasparini, F., Rueegg, D., Stoehr, N., Flor, P. J., Vranesic, I., Prézeau, L., Pin, J. P., Thomsen, C., and Kuhn, R. (1999) CPCCOEt, a noncompetitive metabotropic glutamate receptor 1 antagonist, inhibits receptor signaling without affecting glutamate binding. *Mol. Pharmacol.* **55,** 453–461
45. Chaperon, F., Fendt, M., Kelly, P. H., Lingenhoehl, K., Mosbacher, J., Olpe, H. R., Schmid, P., Sturchler, C., McAllister, K. H., van der Putten, P. H., and Gee, C. E. (2012) Gastrin-releasing peptide signaling plays a limited and subtle role in amygdala physiology and aversive memory. *PLoS One* **7,** e34963
46. Sansig, G., Bushell, T. J., Clarke, V. R., Rozov, A., Burnashev, N., Portet, C., Gasparini, F., Schmutz, M., Klebs, K., Shigemoto, R., Flor, P. J., Kuhn, R., Knoepfel, T., Schroeder, M., Hampson, D. R., Collett, V. J., Zhang, C., Duvoisin, R. M., Collingridge, G. L., and van Der Putten, H. (2001) Increased seizure susceptibility in mice lacking metabotropic glutamate receptor 7. *J. Neurosci.* **21,** 8734–8745
47. Humeau, Y., Shaban, H., Bissière, S., and Lüthi, A. (2003) Presynaptic induction of heterosynaptic associative plasticity in the mammalian brain. *Nature* **426,** 841–845
48. Maurer, T. S., Debartolo, D. B., Tess, D. A., and Scott, D. O. (2005) Relationship between exposure and nonspecific binding of thirty-three central nervous system drugs in mice. *Drug Metab. Dispos.* **33,** 175–181
49. Cryan, J. F., Markou, A., and Lucki, I. (2002) Assessing antidepressant activity in rodents: Recent developments and future needs. *Trends Pharmacol. Sci.* **23,** 238–245
50. Porsolt, R. D. (2000) Animal models of depression: Utility for transgenic research. *Rev. Neurosci.* **11,** 53–58
51. Slattery, D. A., Uschold, N., Magoni, M., Bär, J., Popoli, M., Neumann, I. D., and Reber, S. O. (2012) Behavioural consequences of two chronic psychosocial stress paradigms: Anxiety without depression. *Psychoneuroendocrinology* **37,** 702–714
52. Reber, S. O., Birkeneder, L., Veenema, A. H., Obermeier, F., Falk, W., Straub, R. H., and Neumann, I. D. (2007) Adrenal insufficiency and colonic inflammation after a novel chronic psycho-social stress paradigm in mice: Implications and mechanisms. *Endocrinology* **148,** 670–682
53. Toth, I., Dietz, M., Peterlik, D., Huber, S. E., Fendt, M., Neumann, I. D., Flor, P. J., and Slattery, D. A. (2012) Pharmacological interference with metabotropic glutamate receptor subtype 7 but not subtype 5 differentially affects within- and between-session extinction of Pavlovian conditioned fear. *Neuropharmacology* **62,** 1619–1626
54. Fanselow, M. S. (1980) Conditioned and unconditional components of post-shock freezing. *Pavlov. J. Biol. Sci.* **15,** 177–182
55. Lee Ok, Lee, C. J., and Choi, S. (2002) Induction mechanisms for L-LTP at thalamic input synapses to the lateral amygdala: Requirement of mGluR5 activation. *Neuroreport* **13,** 685–691
56. Rodrigues, S. M., Bauer, E. P., Farb, C. R., Schafe, G. E., and LeDoux, J. E. (2002) The group I metabotropic glutamate receptor mGluR5 is required for fear memory formation and long term potentiation in the lateral amygdala. *J. Neurosci.* **22,** 5219–5229
57. Wootten, D. L., Simms, J., Hay, D. L., Christopoulos, A., and Sexton, P. M. (2010) Receptor activity modifying proteins and their potential as drug targets. *Prog. Mol. Biol. Transl. Sci.* **91,** 53–79
58. Yan, F., Mosier, P. D., Westkaemper, R. B., and Roth, B. L. (2008) Gα-subunits differentially alter the conformation and agonist affinity of κ-opioid receptors. *Biochemistry* **47,** 1567–1578
59. Pelkey, K. A., Lavezzari, G., Racca, C., Roche, K. W., and McBain, C. J. (2005) mGluR7 is a metaplastic switch controlling bidirectional plasticity of feedforward inhibition. *Neuron* **46,** 89–102
60. Pelkey, K. A., Topolnik, L., Lacaille, J. C., and McBain, C. J. (2006) Compartmentalized Ca^{2+} channel regulation at divergent mossy-fiber release sites underlies target cell-dependent plasticity. *Neuron* **52,** 497–510
61. Pelkey, K. A., and McBain, C. J. (2008) Target-cell-dependent plasticity within the mossy fibre-CA3 circuit reveals compartmentalized regulation of presynaptic function at divergent release sites. *J. Physiol.* **586,** 1495–1502
62. Rosemond, E., Wang, M., Yao, Y., Storjohann, L., Stormann, T., Johnson, E. C., and Hampson, D. R. (2004) Molecular basis for the differential agonist affinities of group III metabotropic glutamate receptors., *Mol. Pharmacol.* **66,** 834–842
63. Goddyn, H., Callaerts-Vegh, Z., Stroobants, S., Dirikx, T., Vansteenwegen, D., Hermans, D., van der Putten, H., and D'Hooge, R. (2008) Deficits in acquisition and extinction of conditioned responses in mGluR7 knockout mice. *Neurobiol. Learn. Mem.* **90,** 103–111